FLOW AND HEAT TRANSPORT IN SLOTTED CHANNELS WITH OBSTACLES

É. Ya. Kernerman and V. E. Nakoryakov

We study the flow conditions in narrow channels with obstacles of various shapes at small and moderate Reynolds numbers. The observed flow conditions are compared with experimental data on heat transfer in a channel with obstacles.

Flow and heat transfer in two-dimensional channels with retardation due to sections of bluff bodies have been studied in a comparatively large number of papers. Basically the two-dimensional problem of flow past a cylinder, a plate, a step, and a ditch was studied, i.e., the channel width was sufficiently large that the side walls did not introduce significant distortions in the flow pattern.

But there is considerable practical interest in the flow in laminated heat exchangers with various insertions and cutouts to intensify heat transfer, in the transverse blowing in pipes with thick ribbing, the flow past a flame stabilizer in combustion chambers, in two-dimensional channels of modern radio-electronic devices with blocked grouping of the apparatus, etc.

Information on the flow and heat transfer conditions in narrow channels when the side walls play a significant role in the formation of the velocity field and heat transfer at an obstacle is very contradictory. Some authors assume the formation of dead zones behind the bluff body and, accordingly, a sharp reduction in the heat transfer from the surface of the body and the plates bounding it [1, 2]. But in other papers [3,5] it is stated that the presence of such bodies in the channels leads to additional turbulence in the flow and an intensification of the heat transfer.

These conclusions are based on experimental study of heat transfer in various types of heat exchangers and the results differ markedly depending on the configuration of the model being investigated, the experimental arrangement, and the method of analyzing the results. Also, the pattern of the flow past an obstacle has been little studied. The exception is the theoretical work of Hele-Shaw, Stokes, and Riegels [6-8] in which the flow in a two-dimensional narrow channel past a single obstacle of various shapes at low Reynolds numbers was studied

$$R^* = \frac{U_\infty L}{\nu}\left(\frac{h}{L}\right)^2$$

Here R* is the reduced Reynolds number; U_∞ is the velocity of the fluid at infinity, m/sec; 2h is the distance between the side walls forming the channel, m; L is the dimension defining the obstacle, m; ν is the coefficient of kinematic viscosity, $m^2 \cdot sec$.

To study the flow pattern in the region of moderate and large values of R* an apparatus was prepared similar to that described in [8]. The basic element of the apparatus is a two-dimensional channel with transparent walls of polarized glass of thickness 8 mm. The dimensions of the channel were: length a = 500 mm, width b = 100 mm, distance between side walls 2h was 1.4 and 2 mm.

The body to be investigated was tightly clamped between the walls of the channel and occupied 50 to 80% of its cross section.

Translated from Zhurnal Prikladnoi Mekhaniki i Tekhnicheskoi Fiziki, No. 1, pp. 115-118, January-February, 1971. Original article submitted April 15, 1970.

Fig. 1

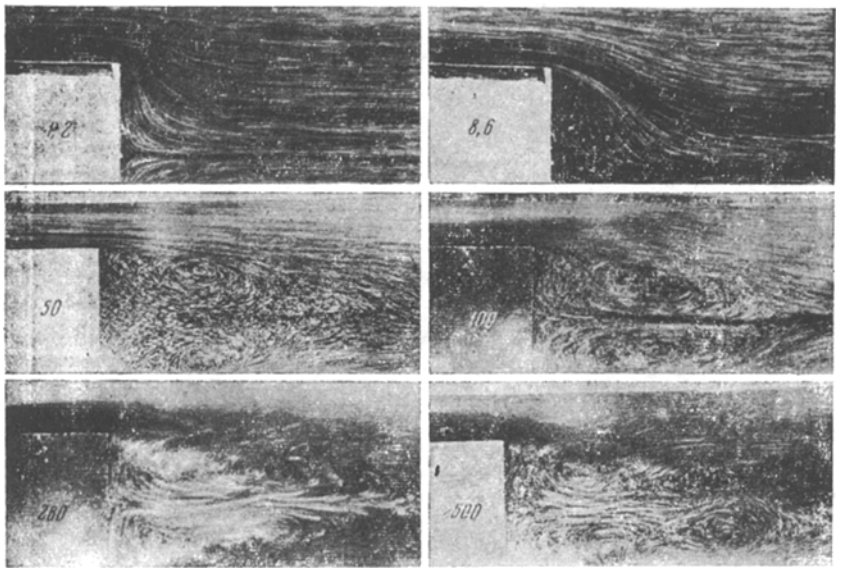

Fig. 2

Water from an intake collector flows uniformly over the whole cross section of the channel. The fluid flow rate was measured with an RS-7 rotameter (accuracy class 2.5). The average fluid velocity in the channel $\langle U \rangle$ was determined by scaling and was changed in the course of the experiment from 0.3 to 7 m/sec. The flow was visualized by introducing aluminum powder diluted by alcohol, into the intake collector.

The use of fine particles of aluminum powder instead of soluble dyes as in [8] made it possible to observe and photograph the flow breakaway and the vortex formation.

With the apparatus described above, the five types of obstacles shown in Fig. 1 were investigated: cylinder, plate, step, ditch, and a series of ditches. The mirror camera "Start" with an adaptor ring was used to take the photographs. Optimum definition of the tracks was achieved by varying the rate of shutter release in inverse proportion to the fluid velocity. The brightness of the lighting apparatus was 1 kW.

To analyze and compare the results of the experiment with those of other papers we have to choose the defining length and the criteria for hydrodynamic similarity. We consider two limiting cases.

1. We assume $h \ll L$. Considering the Reynolds criterion as the ratio of the inertia force F_i to the friction force F_f in the Navier-Stokes equation and estimating the remaining terms, we have for this ratio

$$\frac{F_i}{F_f} = \frac{\rho\,(u\,\partial u/\partial x + v\,\partial u/\partial y)}{\mu\,\partial^2 u/\partial z^2} \sim \frac{\rho U_\infty^2/L}{\mu U_\infty/h} = \frac{U_\infty L}{\nu}\left(\frac{h}{L}\right)^2 \qquad (1)$$

Here x, y, z are rectangular coordinates, the origin being at the intersection of the channel axis with the body; u, v are the velocity components along the coordinate axes, m/sec; ρ is the fluid density, kg · sec^2/m^4; μ is the coefficient of dynamic viscosity, kg · sec/m^2.

It should be noted that this estimate holds throughout the region under investigation with the exception of a small zone at the surface of the body when the derivatives $\partial^2 u/\partial x^2$ and $\partial^2 u/\partial y^2$ cannot be neglected.

2. We assume h is of the same order as L. Similar comparison of the inertia force and the friction force leads to the familiar relation $R = U_\infty L/\nu$.

It is quite obvious that this criterion completely characterizes the flow conditions of the fluid in the fundamental part of the flow. Equation (1) remains valid for the boundary layer at the side walls, but h must be replaced by the thickness δ (x, y) of the boundary layer.

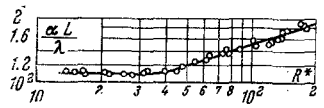

Fig. 3

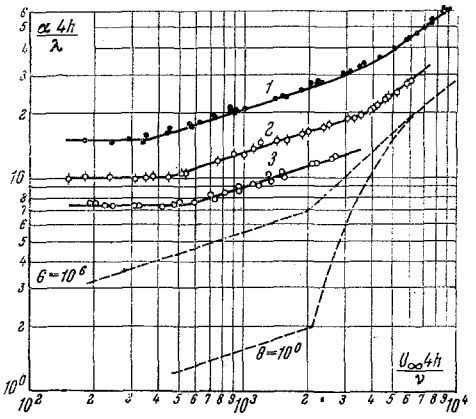

Fig. 4

The thickness $\delta(x, y)$ is determined by the external flow, i.e., the value of $U_\infty L/\nu$, and so the flow conditions at the wall no longer depend on the nondimensional variable h/L. The problem of the upper limit of application of (1) for the flow characteristics has to be determined experimentally in this case. We can assume that this limit corresponds to a value of h/L of the order of unity.

To use (1) we took the defining length L as the transverse dimension of the obstacle (Fig. 1) and the dimension h was replaced by 4h by analogy with the defining dimension of slotted channels.

Figure 2 shows the fluid flow pattern past a rectangular plate for various values of R*. We can distinguish three typical forms of the flow directly at the rear of the plate:

1) laminar flow ($R^* \leq 5$). For $R^* \leq 5$ the flow has an explicit "creeping" character similar to that considered in [6-8]. The velocities between the side walls are distributed in accordance with a parabolic law. Some breakaway is observed only at the sharp edge and is purely local.

2) flow in the dead zone ($5 \leq R^* \leq 40$). As R* increases the rapidly flowing particles in the plane z = 0 are deflected from the body more strongly than the slowly moving particles near the walls. Hence the streamlines of particles at the walls still continue to be of a "creeping" character, while the rapidly moving particles, breaking away from the body reach a region of increased pressure and gradually slow down.

A dead zone is formed behind the plate in which the velocities are very small. The length of this zone gradually increases, and when R* = 40 it is K = 1.5L;

3) flow with vortex formation ($R^* > 40$). As the reduced Reynolds number increases further a reverse flow develops in the dead zone, and at a distance of L/2 from the body two symmetric vortices are formed. The vortices gradually extend and when R* = 150 they occupy almost the whole of the dead zone; the velocity of the reverse flow increases. When $R^* > 150$ the vortices lose stability and mix with each other. This mixing gradually increases and when $R^* > 300$ there is a transition to vortex motion with an explicit Karman wake.

Study of the flow behind a ditch led to similar results. For the case of a step and a cylinder, laminar flow persists up to values of R* equal to 100 and 200, respectively.

Comparison of conditions (A) in which there is no flow breakaway and a dead zone is formed with conditions (B) in which vortices are formed, and also with the results of experiments on heat transfer from the channel walls to the air behind a rectangular plate of thickness 2h = 2 mm and transverse dimension L = 60 mm is given in Fig. 3.

The coefficient of heat transfer α in the Nusselt criterion is defined as the arithmetic mean of the local values of the heat transfer coefficient at 24 points of the surface of the channel behind the obstacle. The temperature of the surface and of the air were measured by a copper-constantan thermocouple of diameter 0.1 mm using a mirror millivoltmeter of type M-95.

We see from Fig. 3 that the flow with no breakaway and the flow with dead zone formation are characterized by a constant value of the heat transfer coefficient which approximates the minimum value of the heat transfer in a two-dimensional channel (Nusselt number Nu = 7.6).

When $R^* > 40$, i.e., when vortices are formed and grow in the region of reverse flow, the heat transfer coefficient increases, the exponent of the power in the heat transfer equation becomes equal to 0.33, which is typical of laminar flow in channels.

Figure 4 gives data on heat transfer behind a flat plate when the distance 2h changes from 2 to 8.6 mm. Here the dotted line indicates the corresponding value of the heat transfer for motion in a slotted channel without obstacles from the data of [9].

It follows from the graphs that the coefficient of heat transfer not only does not decrease when there are obstacles, but conversely, it increases.

We must recall that the pressure head losses also increase and the air temperature in the region of reverse flow rises. This is particularly apparant in very narrow channels and at small velocities. In particular, this can explain the negative effect of obstacles in pipes with thick ribbing, as mentioned at the beginning of the paper. But the situation improves sharply as the distance between the plates increases, particularly when the motion behind the obstacle becomes turbulent, which corresponds to an increase in the slope of the curves 1 and 2 (Fig. 4).

The results of thermal experiments in which the distance between the walls varied can be generalized in the single equation

$$\frac{\alpha 4h}{\lambda} = c\left(\frac{U_\infty 4h}{\nu}\right)^m \left(\frac{4h}{L}\right)^{1/2(m+1)} \tag{2}$$

Here c and m are numerical coefficients.

In the horizontal part of the curves 1, 2, and 3, Eq. (2) becomes

$$\frac{\alpha 4h}{\lambda} = c_1\left(\frac{4h}{L}\right)^{1/2} \quad \text{for} \quad \frac{U_\infty 4h}{\nu}\left(\frac{4h}{L}\right)^{1/2} < 160 \tag{3}$$

i.e., the heat transfer coefficient is independent of the velocity and to a lesser degree depends on the distance between the walls than for motion in the absence of obstacles.

In the second part of the curves, Eq. (2) can be transformed to

$$\frac{\alpha L}{\lambda} = c_2\left(\frac{U_\infty L}{\nu}\right)^{1/2} \quad \text{for} \quad 160 < \frac{U_\infty 4h}{\nu}\left(\frac{4h}{L}\right)^{1/2} < 1600 \tag{4}$$

In this region the heat transfer coefficient is independent of the distance between the walls. This confirms the earlier proposition that the flow conditions at the walls are determined by the flow in the middle of the channel.

When

$$\frac{U_\infty 4h}{\nu}\left(\frac{4h}{L}\right)^{1/2} > 1600$$

the flow is turbulent and the heat transfer coefficient is now a strict function of the distance between the walls since the latter affects the degree of turbulence of the flow in the region near the walls. The exponent of the power in (2) approaches 0.8, which is typical of turbulent fluid motion in smooth channels.

LITERATURE CITED

1. V. M. Buznik, V. N. Bandura, et al., "Investigation of heat transfer and drag for plates with a single element of roughness of various heights. Shipbuilding and marine considerations," in: Republic Interdepartmental Scientific and Technical Conference [in Russian], No. 4, Izd. Khar'kovsk. Un-ta, Khar'kov (1966).
2. F. F. Bogdanov, A. I. Korshakov, and O. I. Utkin, "The intensification of heat transfer in channels," Atomnaya Énergiya, 22, No. 6 (1967).
3. Yu. V. Petrovskii and V. G. Fastovskii, Modern Effective Heat Exchangers [in Russian], Gosénergoizdat, Moscow-Leningrad (1962).
4. P. I. Puchkov and O. S. Vinogradov, "The investigation of heat transfer and the hydraulic drag of annular channels with heat transfer from the internal surfaces," Teploénergetika, No. 10 (1964).
5. N. N. Norkin and I. P. Chashchin, "Heat transfer from tubular surfaces with narrow ribs," Teploénergetika, No. 6 (1961).
6. H. S. Hele-Shaw, "Investigation of the nature of the surface of water and of streamline motion under certain experimental conditions," Trans. Inst. Nav. Arch., 15, p. 25 (1898).
7. G. G. Stokes, "Mathematical proof of the identity of the streamlines obtained by means of a viscous film with those of a perfect fluid moving in two dimensions," Brit. Assoc. Rep. (1898).
8. F. Riegels, "Zur Kritik des Hele-Shaw Versuchs," Z. Angew Math. und Mech., Bd. 18, H. 2 (1938).
9. M. A. Mikheev and I. M. Mikheeva, A Short Course in Heat Transfer [in Russian], Gosénergoizdat, Moscow-Leningrad (1961).